European Journal of Pharmaceutics and Biopharmaceutics 202 (2024) 114412

Contents lists available at ScienceDirect

European Journal of Pharmaceutics and Biopharmaceutics

journal homepage: www.elsevier.com/locate/ejpb

Polymeric nanoparticles produced by electrohydrodynamic atomisation for the passive delivery of imatinib

Scheilly L. Tsilova [a], Benjamin E. Schreiber [b], Rebecca Lever [a], Maryam Parhizkar [a,*]

[a] School of Pharmacy, University College London, London, United Kingdom
[b] National Pulmonary Hypertension Service, Royal Free London NHS Foundation Trust, Pond Street, London, NW3 2QG, United Kingdom

ARTICLE INFO

Keywords:
Nanoparticles
Imatinib
PLGA
Controlled Release
Antiproliferative
Electrohydrodynamic atomisation

ABSTRACT

Imatinib is a chemotherapeutic agent known to cause severe side effects when administrated systemically. Encapsulating imatinib in co-polymer poly(lactic-co-glycolic acid) (PLGA) nanoparticles (NPs) offers a targeted drug delivery. In this work, PLGA 50:50 and PLGA 75:25 NPs encapsulated imatinib using the electrohydrodynamic atomisation technique. All particles generated were spherical with a smooth surface with a size distribution of 455±115 nm (PLGA 50:50) and 363±147 nm (PLGA 75:25). Encapsulation of imatinib was shown to be higher than 75 % and was shown to increase the zeta potential of the loaded NPs. The release of imatinib showed an initial burst in the first 12 h, followed by different sustained releases with up to 70 %. Both types of imatinib-loaded NPs' effect on cell viability and their cellular uptake were also studied on A549 cells, and the antiproliferative effect was comparable to that of cells treated with free drugs. Finally, Rhodamine-B-loaded NP-treated cells demonstrated the cellular uptake of NPs.

1. Background

Imatinib is a chemotherapeutic small molecule acting as a tyrosine kinase inhibitor. It was considered a revolutionary treatment for chronic myeloid leukaemia and was approved by the Food and Drug Administration (FDA) and marketed by Novartis for this indication in 2001 [1]. Imatinib has been researched for its potential to treat several types of cancer [2] and is usually administrated orally; however, the effectiveness of this route and, ultimately, the resulting oral bioavailability highly depends on the physiochemical properties of the drug, such as aqueous solubility, permeability and stability, drug metabolism and the target site [3]. The clinical potential of imatinib is therefore limited by its safety profile, low solubility in aqueous solution and short half-life (~18 h) when administrated orally [4], which leads to a drug concentration that is toxic to normal cells but marginally effective in treating cancer cells [5]. Therefore, an alternative delivery system must be considered depending on the drug's nature and target to achieve optimal bioavailability and efficacy.

Targeted drug delivery provides localised delivery of therapeutics to the affected cells by improving bioavailability, reducing drug distribution to other organs and tissues, and minimising systemic toxic effects [6]. Lipid nanoparticles have been studied to encapsulate imatinib in solid-lipid nanoparticles [4] or lipid nanocapsules [7]. These nanosystems allow for the encapsulation of poorly water-soluble or high-risk drugs and increase their concentration and retention time only at a specific location when administered. Their passive delivery can be achieved by taking advantage of the enhanced permeability and retention (EPR) effect observed in tumour tissues: the lymphatic drainage is reduced, which prolongs the circulation time of nanosized compounds, enough for them to leak into the tumour tissue through the permeable tumour vasculature and then retained in the targeted tissues [8]. Several studies investigating this mode of drug delivery have looked at poly (lactic-co-glycolic acid) (PLGA), an FDA-approved biodegradable polymer. Polymeric drug delivery systems, especially for anti-cancer drugs, show improved storage stability and a more sustained and controlled delivery of their compounds [9]. Imatinib has already been investigated in a PLGA-based drug delivery system, whereby Benny et al (2009) developed imatinib-loaded PLGA microspheres to treat glioblastoma. They injected microspheres intracranially into a glioblastoma mouse model, which led to a 79 % decrease in tumour volume 14 days after the injection [10]. Imatinib-loaded PLGA microspheres were also studied for the treatment of a further type of brain tumour, craniopharyngioma, where a rat corneal angiogenesis assay was utilised, and the imatinib-loaded microspheres were found to reduce neovascularization [11].

* Corresponding author at: 29-39 Brunswick Square, London, United Kingdom.
E-mail address: maryam.parhizkar@ucl.ac.uk (M. Parhizkar).

https://doi.org/10.1016/j.ejpb.2024.114412
Received 12 April 2024; Received in revised form 25 June 2024; Accepted 12 July 2024
Available online 14 July 2024

Imatinib has also been encapsulated to address conditions such as the vascular smooth muscle proliferation in atherosclerosis and pulmonary arterial hypertension. Esfandyari-Manesh et al (2020) showed a controlled release of imatinib from peptide-functionalised PLGA NPs developed for the targeted treatment of atherosclerotic regions [12]. Nakamura et al (2015) demonstrated significant inhibition of smooth muscle cell proliferation 24 h after administrating the loaded NPs intratracheally on a rat model of pulmonary hypertension [13]. The previously mentioned studies used costly and time-consuming multi-step processes that can lead to increased risk of errors, unwanted interaction with the drug, polydisperse and large particles, and low encapsulation efficiency. Electrohydrodynamic atomisation or electrospray (ES) is a one-step technique to fabricate micro and nano-systems [14]. The formation of particles relies on atomising a liquid under an electrical field. The manufacturing is simple and inexpensive, with mild preparation conditions such as the absence of surfactants, emulsifiers, and high temperatures [15].

Electrospraying also allows great flexibility in the type of materials used and control over the resulting products and their characteristics [16]. Production of PLGA NPs using electrospraying has shown its potential in many studies for reducing severe side effects and localised drug delivery; for instance, metronidazole was encapsulated using ES due to its carcinogenicity concerns [17]. A study by Parhizkar et al (2016) electrosprayed PLGA nanoparticles encapsulating the anti-cancer drug cisplatin for a controlled dosage and release [18]. Studies by Xie et al (2006) and Chatterjee et al (2020) electrosprayed Paclitaxel and methotrexate NPs, respectively, looked to minimise systemic exposure and ensure a high concentration reaching the brain for malignant glioma [19] or drug-resistant metastatic breast cancer cells [20] respectively.

This study aimed to create and evaluate polymeric NPs produced through electrospray technology to achieve a more precise and efficient delivery of imatinib for improved dosing effectiveness. This involved manufacturing nanoparticles using electrospraying and optimising them for size, shape, composition, and morphology for optimal delivery. The resulting NPs were characterised to ensure they carry the desired properties to deliver imatinib effectively; this included evaluating drug encapsulation efficiency and drug release profile in vitro. Finally, the resulting nanoparticles were tested on A549 cells to assess their efficacy in vitro.

2. Methods

Imatinib-loaded nanoparticles and Rhodamine-B loaded nanoparticles (RhD-B NPs) production and characterisation

Materials.

The co-polymer poly(lactic-co-glycolic acid) (PLGA) was used to fabricate the nanoparticles with a ratio of lactide to glycolide of 50:50 and 75:25, also known as Purasorb PDLG 5002 and Purasorb PDLG 7502 respectively; with the molecular weight of 17 000 g/mol, and the inherent viscosity at 0.2 dl/g. The copolymer was purchased from Corbion Purac. Acetone and methanol were purchased from Sigma-Aldrich, and dimethylacetamide (DMAc) was purchased from Fisher Chemical. The chemotherapeutic agent, imatinib, was purchased from Cambridge Bioscience. Rhodamine-B (RhD-B) was purchased from Sigma-Aldrich. BioDesign Cellulose Dialysis Tubing Strips, 14000 MWCO, were purchased from ThermoFisher Scientific and phosphate-buffered saline (PBS) tablets were purchased from MP Biomedicals, Inc.

Production of NPs.

All polymer solutions were prepared with 2 wt% PLGA. Formulations F1, F2, F3, F4 dissolved the PLGA using a co-solvent system of acetone and DMAc, with a ratio of 1:1 and formulations F5, F6, F7, F8 dissolved PLGA using DMAc alone. Imatinib (0.2 wt%) was added to F2, F4, F6, and F8 to produce drug-loaded nanoparticles. F1, F3, F5, and F7 were prepared without the drug as blanks, and RhD-B (0.2 wt%) was added to F9 to produce rhodamine-loaded NPs (RhD-B NPs). Formulations F1, F2, F5, F6 and F9 were made using PLGA 50:50 and F3, F4, F7 and F8 were made using PLGA 75:25. Droplets of polymer solutions were ejected out of a 22G (ID: 0.41 mm and OD: 0.72 mm) needle under a constant flow rate of 5 μL/min and at a voltage of 12 kV for F1, F2, F3, and F4 and 2 μL/min and 14 kV for F5, F6, F7, F8, F9. A voltage power supply applies an electrical field to the needle to break the droplet's surface tension and create smaller droplets. While the droplets migrate towards the collector, they separate into smaller droplets, and the solvent evaporates, generating dry small particles on the collection plate [21]. Electrospraying occurred at room temperature (20–25 °C) and 35–55 % relative humidity. A summary of all the parameters is displayed in Table 1.

Characterisation of NPs.

The morphology and porosity of the NPs were studied using scanning electron microscopy. The electrosprayed particles were collected on a microscope slide, then cut and attached to aluminium SEM stubs using a double-sided carbon sticker (TAAB Laboratories, UK). The stubs were then gold-coated for 1 min to make the sample conductive for observation under scanning electron microscopy (Thermo Scientific Phenom Pro G6 Desktop SEM) with an acceleration voltage of 15 kV. Formulations F1-F8 were each electrosprayed on three separate occasions to demonstrate the reproducibility of the technique, and the image processing software ImageJ (NIH, USA) was used to determine the particle size distribution using the software-embedded functions on three separate images. Zeta potential of the imatinib-loaded and blank particles and pure imatinib were also measured using a Nano ZetaSizer (Malvern Panalytical) and results were statistically compared using one-way ANOVA.

Fourier transform infrared spectroscopy.

Fourier transform infrared (FTIR) spectroscopy (PerkinElmer Spectrum 100 FT-IR) was conducted with spectra recorded in the wavelength region of 4000 to 650 cm^{-1}. Pure imatinib, blank particles and imatinib-loaded particles from different PLGA ratios were dispersed on the crystal light path and compressed to obtain respective spectra. A background scan was performed, followed by a sample scan. Both scans consisted of 8 scan times, and each sample was run in triplicates to confirm the spectra.

Encapsulation efficiency (EE%).

A calibration curve was generated for imatinib encapsulation efficiency by dissolving a range of concentrations of imatinib (20–640 μg/ml) in a co-solvent mixture of Acetone and DMAc (9:1) and measuring their absorbance at a wavelength of 332 nm using a UV–Vis Spectrophotometer (Cary Series UV–Vis Spectrophotometer, Agilent Technology). Encapsulation efficiency was determined by using the calibration curve and measuring the absorbance of the dissolved imatinib-loaded particles at the same wavelength of 332 nm using a UV–Vis Spectrophotometer.

In-vitro drug release profile.

A release study measured the percentage of imatinib released in PBS over 7 days. PBS is a United States Pharmacopeia (USP) standard physiological buffer for replicating the human body's pH, osmolarity, and ion concentration to simulate the conditions in-vivo [22], but also due to its studied effect on drug release from PLGA microparticles [23]. 8 mg of Imatinib-loaded particles and 1 mg of pure Imatinib were suspended in dialysis bags. Aliquots were withdrawn at specific time points, every 2 h during the first day and every 24 h after that until day 7. The aliquots were passed through a 0.22 μm filter. UV absorbance of the resulting filtrates was then measured at 261 nm. The imatinib concentration of each aliquot was determined using the release study calibration curve, generated by dissolving a range of concentrations of imatinib (2–50 μg/ml) in a co-solvent mixture of PBS and methanol (4:1) and measuring their absorbance at a wavelength of 261 nm.

Cell studies.

Materials.

A549 cells were purchased from PromoCell and grown in Dulbecco's Modified Eagle Medium (DMEM), supplemented with 10 % fetal bovine serum and 1 % penicillin–streptomycin. Media, supplements and

Table 1
Nanoparticles (NPs) production parameters.

Formulations	Polymer Solution properties					Electrospraying processing parameters	
	PLGA concentration	PLGA ratio	Drug used and concentration		Solvents	Voltage	Flow rate
F1	2 wt%	50:50	Imatinib	0	Acetone and DMAc (1:1)	12kv	5 μL/min
F2				0.2 wt%			
F3		75:25		0			
F4				0.2 wt%			
F5		50:50		0	DMAc	14kv	2 μL/min
F6				0.2 wt%			
F7		75:25		0			
F8				0.2 wt%			
F9		50:50	Rhodamine-B	0.2 wt%			

Phosphate-buffered saline (PBS) were purchased from ThermoFisher. CellTiter 96 ® Non-Radioactive Cell Proliferation Assay (MTT) was purchased from Promega and LIVE/DEAD™ Cell Imaging Kit (488/570) from ThermoFisher.

Cell viability and live/dead assay.

Imatinib-loaded NPs were assessed following F6 and F8 (PLGA 50:50 and 75:25, DMAc, 2 μL/min), on A549 cell lines due to their size and release profile with their respective blanks. Cell viability was measured

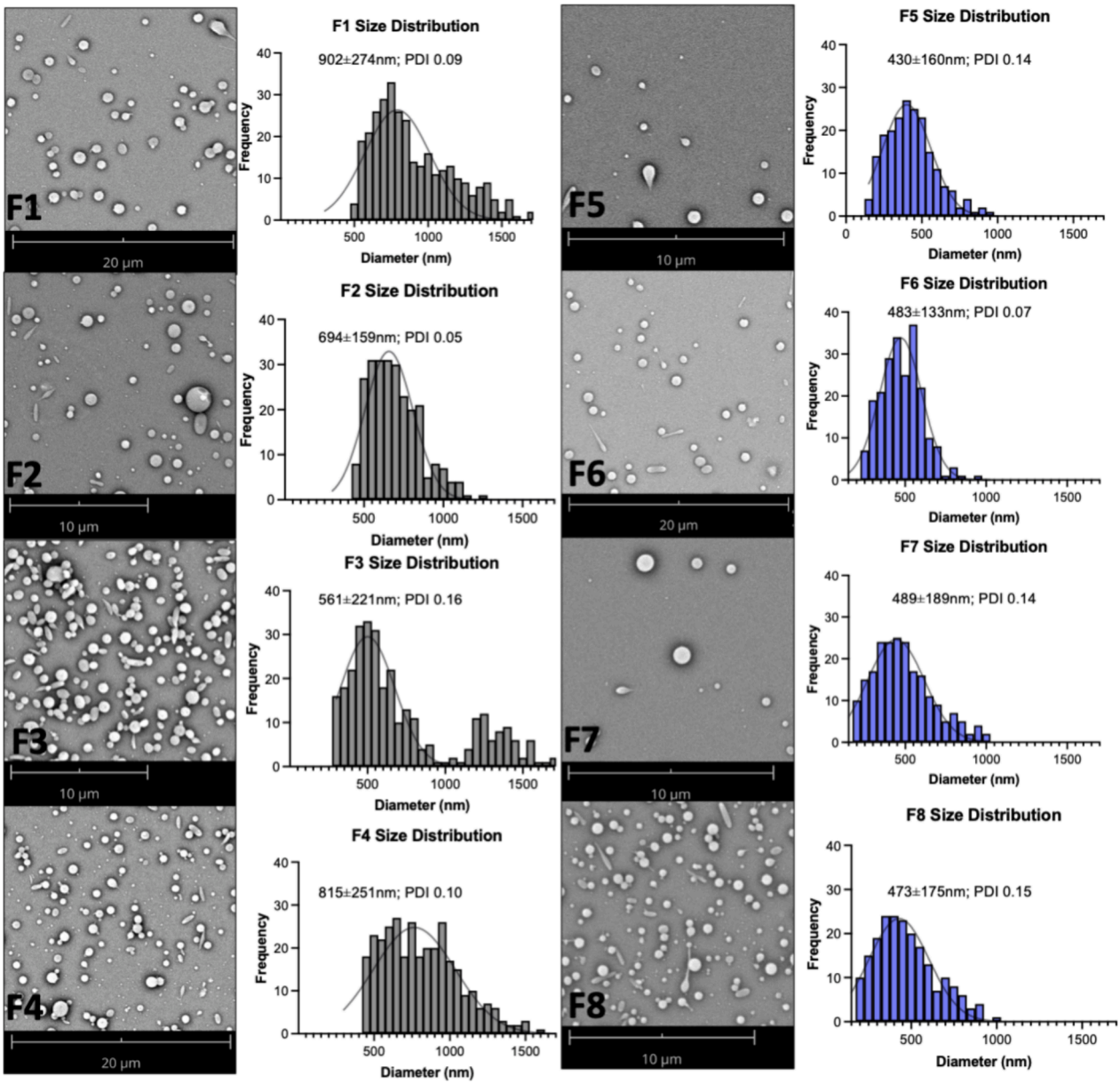

Fig. 1. Scanning Electron Microscope (SEM) images of all formulations of NPs with their respective size distribution and PDI. Data are expressed as the mean +/- s.e. mean of 3 independent experiments carried out in triplicates.

using a colorimetric MTT assay. A live/dead assay was also performed. 96-well plates were seeded with 2000 cells in each well and treated the next day with media alone (untreated), F5 NPs and F6 NPs (both at 1 mg/ml) and a range of imatinib concentrations of 50 μM, 100 μM, and 150 μM. MTT assay was conducted 72 h after the cells were treated, and the absorbance was measured on a SpectraMax absorbance multi-well plate reader at 550 nm, following the manufacturer's instructions. The live/dead assay contains Calcein AM, a cell-permeant dye that stains green live cells, and BOBO-3 iodide, which stains red dead cells. 72 h after treating the cells, they were washed and stained with both dyes. Qualitative images were taken using an EVOS fluorescence microscope 30 min after adding the dyes. The fluorescence signal was measured on a SpectraMax absorbance plate reader at emission/excitation 488/515 nm for live cells and 570/602 nm for dead cells.

Uptake study.

A 24-well plate was seeded with A549 cells at a density of 95,000 cells in each well. The uptake study treated cells with media (untreated), F5 NPs, free RhD-B at 50 μg/mL (equivalent to 100 μM free imatinib), and F9 NPs (Blank PLGA 50:50 and Rhodamine-B PLGA 50:50) at 1 mg/mL. One row was left unseeded to serve as an additional negative control to ensure that measurements reflected the interaction of the NPs with the cells rather than the plate. The following day, the wells were rinsed three times with PBS to remove any NPs or RhD-B that were not internalised.

Rhodamine-B fluorescence was measured on a SpectraMax plate reader with an excitation peak at 550 nm and an emission peak at 570 nm, and fluorescent images were obtained using the Invitrogen EVOS Digital Inverted Fluorescence Microscope.

3. Results

Imatinib-loaded particles characterisation

Size and morphology.

The electrohydrodynamic atomisation of the polymer solutions generated individual, smooth, and spherical particles using all formulations in Fig. 1, along with each formulation's respective size distribution, mean size and PDI. All formulations showed a low polydispersity index (all below 0.3) as well as a decreasing mean size in F5 (430 ± 160 nm; PDI 0.14), F6 (483 ± 133 nm; PDI 0.07), F7 (489 ± 189 nm; PDI 0.14), and F8 (473 ± 175 nm; PDI 0.15) compared to F1 (902 ± 274 nm; PDI 0.09), F2 (694 ± 159 nm; PDI 0.05), F3 (561 ± 221 nm; PDI 0.16) and F4 (815 ± 251 nm; PDI 0.10).

Zeta-potential and FTIR.

The surface charge of the particles was measured as it was reported that the charge influenced the particles' effect on cytotoxicity and their cellular uptake [24]. Fig. 2A displays the surface charge of the blank and imatinib-loaded PLGA 50:50 and 75:25 NPs and the charge of imatinib alone. The charge increase in the encapsulated particles indicates that adding imatinib significantly affects the charge of the particles. Indeed, the mean charge of pure imatinib at −9 ± 2 mV is higher than the blank NPs at −21 ± 4 mV (PLGA 50:50) or −17 ± 7 mV (PLGA 75:25) and it is shown that the encapsulation of imatinib in PLGA NPs increases the zeta potential to −13 ± 7 mV (PLGA 50:50) or −15 ± 4 mV (PLGA 75:25). The addition of the drug appeared to influence the surface charge of the particles.

FTIR has been chosen to identify the incorporation of the drug within the polymeric particles. Fig. 2B displays the FTIR spectrum of the pure PLGA 50:50 and 75:25, which yielded the same spectrum as their respective blank PLGA, encapsulated PLGA particles and pure imatinib. The C = O stretch of imatinib can be observed in the encapsulated-PLGA particle spectra in the 1600 cm^{-1}, pointed out by the red circles in both Imatinib-PLGA 50:50 and Imatinib-PLGA 75:25.

Encapsulation efficiency and release profile of Imatinib-loaded NPs.

The encapsulation and release of imatinib in the four different drug-loaded formulations (F2, F4, F6 and F8) were studied and compared to observe the effect of the type of polymer and the effect of solvent on the encapsulation efficiency and release of imatinib. When comparing the effect of the different types of PLGA polymer, the mean encapsulation efficiency for F2 was found to be around 89 ± 4 % and 98 ± 13 % for F6 in PLGA 50:50, and a slight decrease in the mean encapsulation efficiency in F4 with 79 ± 5 % and F8 with 93 ± 9 % using PLGA 75:25, however not significantly different as shown in Fig. 3A. All release profiles in Fig. 3B showed an initial burst release of imatinib in the first 12 h. The burst release in the particles generated from F6 was more significant than in F8, F2 and F4. F6 (483 ± 133 nm) have indeed shown subsequently to release much faster than F8 (473 ± 175 nm), F2 (694 ± 159 nm) and F4 (815 ± 521 nm). Pure imatinib's release is much slower than all the other release profiles and only reaches a release of 16 % after

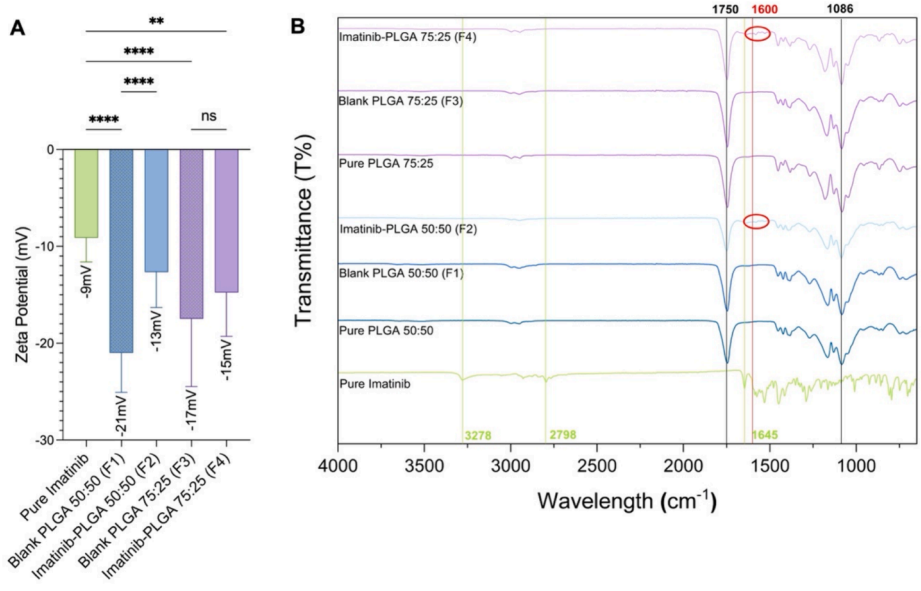

Fig. 2. A. Zeta potential of pure imatinib, blank (F1 and F3) and imatinib-loaded PLGA NPs with PLGA ratio 50:50 (F2) and 75:25 (F4). Data are expressed as the mean +/- s.e. mean of 3 independent experiments, each carried out in triplicates (*P < 0.05, **P < 0.01, ***P < 0.0001; data analysed by one-way ANOVA) and **B.** Corresponding FTIR spectrum with pure PLGA spectrum (50:50 and 75:25). Red circles showing the Imatinib specific amine group in the drug encapsulated PLGA nanoparticles.

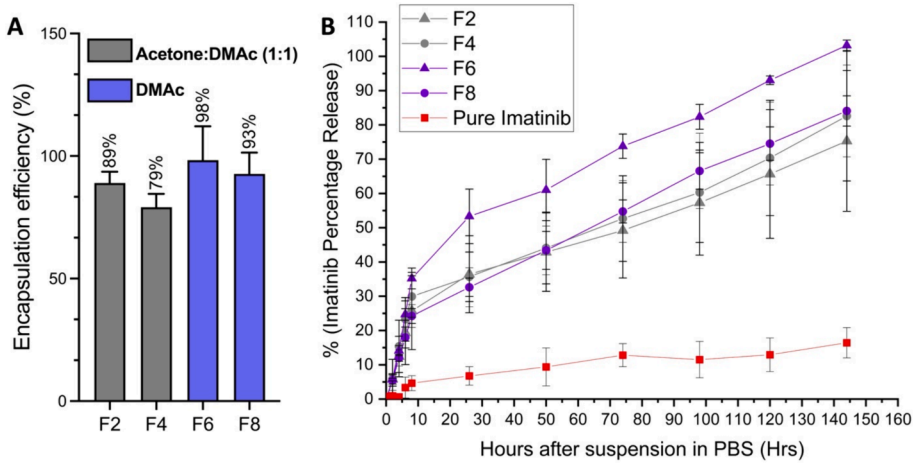

Fig. 3. A. Respective encapsulation efficiency of imatinib in F2, F4, F6, F8 IMA-NPs. **B.** Imatinib percentage release from F2, F4, F6 and F8 IMA-NPs and pure imatinib after being suspended in PBS over seven days. Data are expressed as the mean +/- s.e. mean of 3 independent experiments (*P < 0.05, **P < 0.01, ***P < 0.0001; encapsulation efficiency data analysed by two-way ANOVA).

seven days. Mathematical models have been investigated to predict polymeric particles' drug release and diffusion behaviour, and the obtained release data were fitted to four common models: zero-order, first-order, Higuchi and Korsemeyer Peppas models. Table 2 displays the relevant model equations, with f being the amount of drug released over time t, and R^2 the correlation coefficient, with the latter indicating which model is appropriate for the drug release. Our drug release profiles showed better fit with the Korsemeyer Peppas model with an R^2 of 0.99, 0.98, 0.97 and 0.99 for F2, F4, F6 and F8, respectively.

Effect of the imatinib-loaded NPs (F6 and F8) and RhD-B NPs (F9) on A549 cells.

Cytotoxicity of F5, F6, and F8 NPs on A549 cells.

Formulations F5, F6, and F8 NPs were chosen for the in-vitro cell studies due to their small size, as their delivery relies on the EPR effect in the 100–400 nm range. Our resulting NPs range from 400-500 nm in size. Imatinib IC_{50} was found to be approximately 120μM, which is within the range of the concentrations found in the literature for this cell line of 61 and 150 μM [28,29]. The drug release results obtained from F6 and F8 NPs allowed for the calculation of the dose of NPs that would encapsulate enough imatinib needed to achieve inhibition of proliferation. It was found that a concentration of 1 mg/ml of NPs can release between 120 and 180μM of imatinib within 72 h.

Both assays measure cell viability, either by measuring mitochondrial or cellular enzymatic activities, and both approaches exhibit a reduction in these parameters when cells are treated with the imatinib-loaded NPs and a range of imatinib concentrations alone when compared with the untreated cells (control). Indeed, cell viability has been shown to decrease to 48 ± 11 % and the percentage of live cells to 38 ± 20 % when cells were treated with F6 and a decrease to 57 ± 13 % in cell viability and 25 ± 9 % in the percentage of live cells when treated with F8. These quantitative results are reflected qualitatively in the data shown in Fig. 4. Since it was shown that the type of PLGA did not affect cell viability, only F5 and F6 were tested for the qualitative aspect of the live-dead assay. Fig. 5 displays the qualitative results of the live-dead assay, following treatment of the cells with imatinib-loaded and blank-loaded NPs (F5 and F6) and a range of imatinib concentrations (50, 100, 150 μM), respectively. No visual changes in the green-labelled cells were seen between the untreated cells and F5 (Fig. 5), which indicates no changes in the proportion of live cells when cells are treated with blank PLGA. A concentration-dependent reduction in live cells can be observed when cells were treated with increasing imatinib concentrations. Our imatinib-loaded nanoparticles have shown their efficacy on A549 cells regardless of the type of PLGA used to encapsulate imatinib.

Cellular uptake of F9 NPs into A549 cells.

Here, we investigated the facilitation of imatinib's internalisation in the cells. The fluorescent dye rhodamine-B was used to examine the uptake of the NPs into the cells. The fluorescence was measured in untreated cells and cells treated with blank NPs (F5), which showed little to no fluorescence (Fig. 6). The F9 NPs were added to both cell-seeded and non-seeded wells to ensure that relevant fluorescence measurements reflected the interaction of NPs with the cells and not the tissue culture plate. F9 NPs in non-seeded wells showed no significant difference from those untreated, indicating that NPs not taken up by cells can be successfully rinsed out of the wells. Only the F9 NP-treated wells showed significant fluorescence readings, also higher than free RhD-B, indicating the uptake of rhodamine-loaded NPs into the cells within 24 h.

Table 2
Release kinetics models of Imatinib-loaded NPs.

Kinetic models	Kinetic parameters	F2	F4	F6	F8
Zero-order	K_0	0.693	6.434	1.497	6.752
Eq 1. $f = K_0 t$ [25]	$\mathbf{R^2}$	**0.922**	**0.914**	**0.894**	**0.943**
First-order	K_1	0.011	6.434	1.497	6.752
Eq 2. $\ln(1-f) = K_1 t$ [26]	$\mathbf{R^2}$	**0.949**	**0.938**	**0.919**	**0.960**
Higuchi	K_H	6.093	6.434	9.372	6.752
Eq 3. $f = K_H\sqrt{t}$ [25]	$\mathbf{R^2}$	**0.981**	**0.973**	**0.967**	**0.988**
Korsemeyer Peppas	K	8.784	10.226	9.962	6.877
Eq 4. $f = \frac{M_t}{M_\infty} = Kt^n$ [27]	n	0.409	0.384	0.481	0.493
	$\mathbf{R^2}$	**0.987**	**0.982**	**0.968**	**0.988**

4. Discussion

The use of electrospraying in our study shows its versatility as various particle morphology and size were possible to achieve through the tailoring of the polymer solution and processing parameters, and each parameter has an interdependent influence on the particles' characteristics. For instance, the polymer's molecular weight and concentration can greatly impact the polymer solution characteristics, such as its viscosity and, in turn, its surface tension [30]. Selecting a low polymer concentration of 2 wt% ensured the formation of spherical particles as a higher polymer concentration could generate more elongated particles or non-uniform particles [31] as the increase in concentration led to the rise in viscosity and polymer chain entanglement [32]. For the formation of small and spherical particles, the polymer entanglement in the polymer solution needs to be low as the increase of the entanglement inhibits the droplet fission process [33]. A study on electrospray

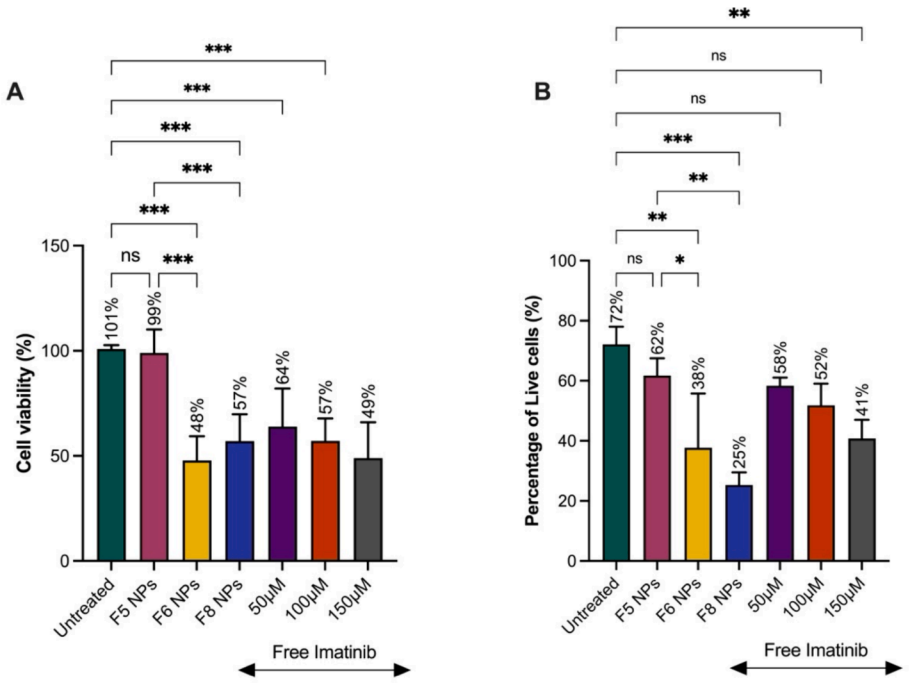

Fig. 4. A. MTT assay results and B. Live/Dead cells ratio, both conducted 72 h after treatment with IMA-NPs and free imatinib. Data are expressed as the mean +/- s. e. mean of 3 independent experiments, each carried out in duplicate (*P < 0.05, **P < 0.01, ***P < 0.0001; data analysed by one-way ANOVA).

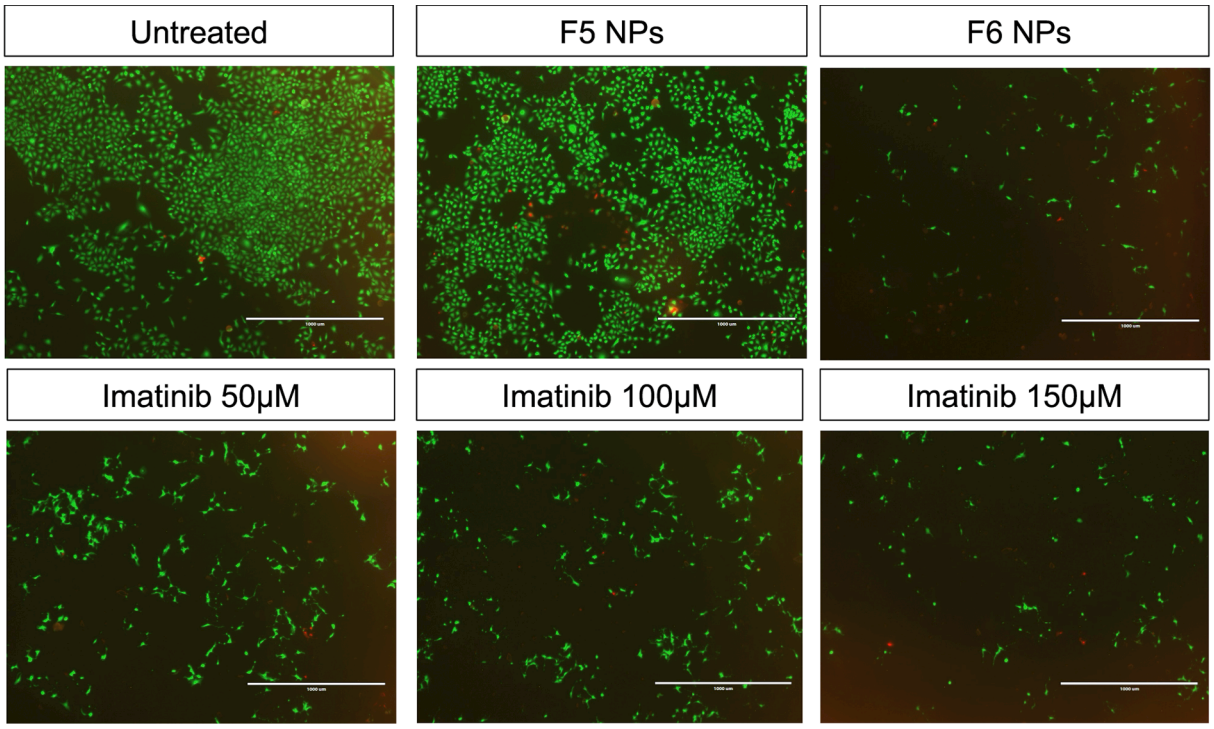

Fig. 5. Live/Dead Assay on A549 cells 72 h after treatment with medium (untreated), F5 NPs (blank), and F6 NPs (imatinib-loaded), both at 1 mg/ml and a range of imatinib concentrations (50, 100, 150 μM). Live cells were stained green with Calcein AM, and dead cells were stained red with BOBO™-3 Iodide.

polycaprolactone NPs encapsulating bosentan monohydrate found that smaller particles were formed as the polymer concentration was reduced [34]. Other parameters of the polymer solution also influence the morphology and size of the produced particles. For instance, the choice of solvent can dictate the evaporation rate, electrical conductivity, viscosity, and surface tension of a polymeric solution [35]. A more volatile solvent evaporates before the particles can further separate into smaller particles, which means the droplets solidify too early and may create larger, irregular, and porous particles [36]. The solvents chosen for this study were acetone and DMAc, with the latter having a higher electrical conductivity, viscosity, and surface tension (37, 38) than acetone, whilst acetone has a higher evaporation rate [9,37]. The binary solvent system of acetone and DMAc for F1, F2, F3 and F4 allowed a higher flow rate of 5 μL/min. A binary solvent system would allow for a balanced solvent

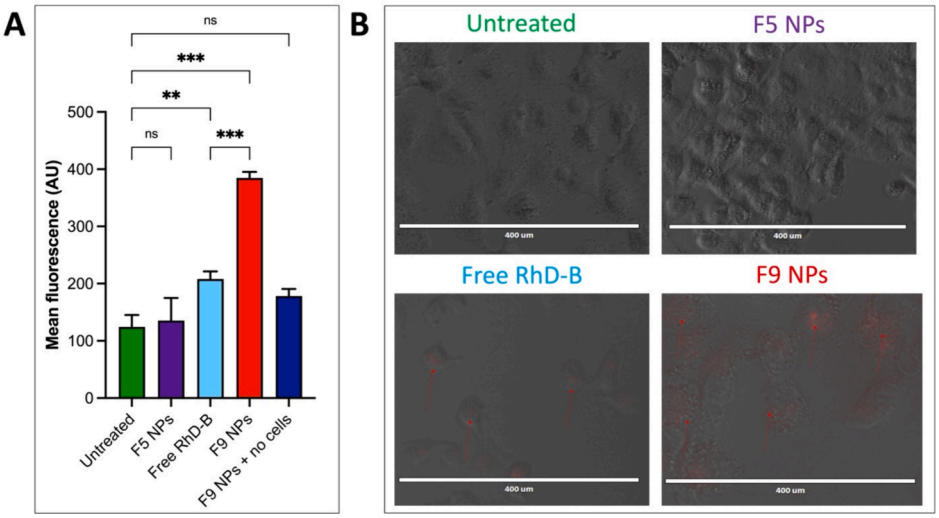

Fig. 6. A. The uptake assay result was obtained 24 h after treating A549 cells with rhodamine-B-loaded NPs. **B.** Corresponding EVOS fluorescence images demonstrating the uptake of RhD-B pointed out by red arrows. Data are expressed as the mean +/- s.e. mean of 3 independent experiments, each carried out in duplicates (*P < 0.05, **P < 0.01, ***P < 0.0001; data analysed by one-way ANOVA).

evaporation rate, allowing droplets to further atomise before reaching the collection plate and ensuring dense, smooth, and completely dried particles are collected. Trotta et al (2010) investigated the effect of different solvents on the production of electrosprayed solid lipid-based particles and found that by using the solvent with a high boiling point, the structure of the particles was stronger, and their morphology was less irregular [38]. In our study, F5, F6, F7, and F8 produced smaller particles than F1, F2, F3, and F4 by further decreasing the evaporation rate of the solvent by removing acetone [39].

Processing parameters such as flow rate and voltage were then adjusted to match the polymer solution characteristics. For instance, the flow rate was also adjusted to the less volatile solvent, DMAc, and reduced from 5 to 2 μL/min. The lower flow rate also produces smaller particles by decreasing the dispensed droplet size, ultimately decreasing the size of the separating droplets. Yao et al (2008) electrosprayed two solutions of PLGA using acetonitrile and dichloromethane at two different concentrations and showed an increase in the particles size from 0.5 μm to 25 μm by increasing the flow rate from 2 to 4 mL/hr in both solutions [40]. The voltage had to be then adjusted to match the new solution and processing parameters, which was increased from 12 to 14 kV as a higher electrical charge can overcome the cohesive forces of the particles and break the droplet into smaller droplets but can also lead to samples with a low polydispersity index [21,41]. Meng et al (2009) looked at the variables in the electrospraying of four different molecular weights of PLGA and the effect of the applied potential and showed a decline in particle diameter when the applied voltage increased [42]. Our study, along with the ones mentioned, showed the potential of electrospraying in the production of particles of various sizes and morphologies but mostly demonstrated the high level of control over the particles' characteristics, making the electrospraying technique highly reproducible, versatile, and flexible.

Our study has also shown that adding imatinib increased the zeta potential of the particles, indicating that imatinib was found partially on the surface of the particles. When the particles are formed through electrospraying, the high voltage applied breaks the initial droplets dispensed by the needle into smaller droplets, which form the particles [43,44]; and as the solvent evaporates, the dry particles travel to the collection plate [45]. During that process, the separation of these droplets can cause some of the drugs to precipitate on the surface of the particles instead of being incorporated in the PLGA matrix, especially in NPs with a high encapsulation efficiency likely due to the polymer reaching saturation with the encapsulated drug; this could explain the increased zeta potential seen in imatinib-loaded particles [46].

Imatinib incorporation within the PLGA particles has been shown through the FTIR spectrum of Imatinib-loaded NPs. Indeed, Imatinib's FTIR spectrum obtained corresponds to the ones found in the literature by Veverka et al (2012), and Bhattacharya (2020) [47,48] and PLGA spectrum by Fu et al (1999) [49]. The FTIR spectrum for both types of pure PLGA has a strong peak at 1086 cm^{-1} and 1750 cm^{-1} indicating a C-O-C and C═O stretching respectively [49]. Imatinib's characteristic peaks can be found at around 3279 cm^{-1} and 2798 cm^{-1} indicating the presence of N–H and carboxylic acid C═O and O—H stretch respectively [47]. The sharp stretches at around 1500 cm^{-1} signify the presence of a C═O stretch and finally, the ones between 1500 to 650 cm^{-1} display the presence of an aromatic group. The addition of imatinib found in the 1600 cm^{-1} indicates its aromatic group however this characteristic peak was significantly reduced in the encapsulated-PLGA spectra [48]. Imatinib is a BCS class I small molecule [47] and was found to be amphiphilic as its chemical structure contains both polar (nitrogen and hydrogen groups) and nonpolar groups (benzene rings and methyl groups), creating a small molecule with hydrophobic and hydrophilic properties [50,51]. The reduction of intensity could be due to hydrophobic interaction between the long carbon chain of PLGA and imatinib's benzene ring, as observed by Liu et al (2021) on their FTIR spectrum of electrospray imatinib and paclitaxel-loaded core–shell microparticles [52]. According to a study by Kumar et al (2021) that investigated the in-silico interaction between imatinib and PLGA, the configuration pattern showed that the hydrogen on imatinib's benzene ring forms a hydrogen bond with PLGA's ester and imatinib's methyl group (CH_3) also forms a hydrogen bond with the ketonic group of PLGA (R—C(═O)—R') [53].

Our study has demonstrated a high encapsulation of imatinib with a slightly lower encapsulation efficiency when using PLGA 75:25. The electrospraying method allows for a high encapsulation of both hydrophobic and hydrophilic drugs, regardless of the hydrophobicity of the polymer. Valo et al (2009) electrosprayed beclomethasone dipropionate, a hydrophobic drug, and salbutamol sulphate, a hydrophilic drug, and showed that the hydrophobicity and hydrophilicity of the drugs did not affect their encapsulation efficiency when electrosprayed [54]. The solvents used for F2 and F4 were DMAc and acetone, and DMAc was only used for F6 and F8. The evaporation rate of acetone is higher than that of DMAc, which can lead to irregular and porous particles when electrosprayed [36]. This could explain the slightly lower encapsulation efficiency in F2 and F4.

The drug release profiles from the particles presented in this study follow a biphasic profile, with the first phase being the initial burst release and the second phase being a slow-release phase (59) compared to the slower release of pure imatinib. The drug release from nanoparticles displayed a greater burst release and faster release from F6 (483 nm). This initial burst release could be due to the heterogeneous distribution of the drug in the polymer matrix during the formation of the particles through electrospraying, as previously mentioned by the increased zeta potential (Fig. 2A) [46,55]. The initial burst release of imatinib can also be attributed to the surface degradation of the particles following the start of PLGA hydrolysis [56]. Drug diffusion, swelling and polymer degradation are the other mechanisms involved in drug release from PLGA drug delivery systems [57,58]. Various common mathematical models were investigated to fit the drug release, such as zero-order, first-order, Higuchi, and Korsmeyer-Peppas. The Korsmeyer-Peppas model was determined to be the best fit and is expressed as $f = \frac{M_t}{M_\infty} = Kt^n$, the amount of drug release f over time t, with K being the kinetic constant incorporating nanoparticles' structures and n the exponent characterising the release mechanism [59]. The drug release mechanism suggests a Fickian diffusion as the calculated exponent n for all formulations was < 0.5 [60]. The Korsemeyer Peppas model has been previously used to evaluate the release of actives from PLGA NPs. For instance, Esmaili et al (2018) encapsulated PLGA NPs for the controlled release of curcumin, and the Korsemeyer Peppas model has also been found to fit the release of the active ($R^2 = 0.90$) and to follow Fickian diffusion ($n = 0.282$) [61]. In the study by Chatterjee et al (2020), the electrosprayed PLGA NPs carrying the anti-cancer treatment methotrexate was also found to fit the Korsemeyer Peppas model ($R^2 = 0.99$) and to follow Fickian diffusion ($n = 0.49$) in their release of the drug [20]. Studies have shown that size and porosity significantly affect the drug release from PLGA-based particles as they affect polymer erosion and drug diffusion [58]. Previous work has shown that smaller particles were associated with faster release. Berkland et al (2002) had demonstrated that the rate of release decreased with the increase in particle size when they looked at rhodamine-B and piroxicam-loaded PLGA microspheres [62]. This is also consistent with the increase in surface area to volume ratio in smaller particles [62], allowing more water to encounter the NPs, contributing to swelling and leading to higher hydrolysing of the polymer, faster diffusion and ultimately a faster release [11,56]. It was also noted that although F6 have a similar size to F8 (473 nm), F6 showed a faster release. This is due to F6 being produced using PLGA 50:50, which has a lower lactic acid to glycolic acid ratio and is the least hydrophobic polymer, which increases the rate of water absorption and hydrolysis, leading to a faster drug release [56] as seen here compared to F8 and as reported in previous studies [63]. Both Benny et al (2009) and Karal-Yalmaz et al (2016) investigated PLGA 50:50, 75:25 and 85:15 for the release of imatinib mesylate and found that PLGA 50:50 released the drug faster than 75:25. Benny et al. (2009) attributed the difference to the higher hydrophobicity of PLGA 75:25 [10] and Karal-Yalmaz et al (2016) to the difference in size where smaller size led to a faster release [11]. Although the literature suggests that larger particles release the drug at a slower rate, the larger particles prepared in this work using F2 (902 nm) and F4 (674 nm) had a similar imatinib release rate to F8 (473 nm). This can be explained as adding acetone in F2 and F4 can lead to more porous NPs and impact its release. Porous PLGA-based microparticles release their content much faster than non-porous PLGA-based microparticles [64] by facilitating the water erosion of the polymer by the broader surface area and increasing the mobility of the drug molecules [65]. The slower release of free imatinib may be due to the low solubility of the free base imatinib [66]. Because of imatinib's low solubility, we do not expect the same release profile experienced by NPs. The encapsulation enabled a controlled release rate of imatinib, which does not rely on imatinib's solubility; its release may also be controlled by changing the NP characteristics, in this case, the size and porosity of the NPs [67]. Overall, Imatinib was released faster in this work than in other studies such as Karal-Yilmaz et al (2016; 35 days) or Benny et al (2009; 30 days). It has been shown that a faster release has been associated with higher drug content. A study by Zhang et al (2018) achieved close to 100 % release of progesterone from electrosprayed PLGA particles in approximately one week with an encapsulation efficiency of 83 % [68].

Our in-vitro cell viability results show decreased cell viability and live-cell ratio following treatment with free imatinib and imatinib-loaded NPs (F6 and F8). These results are consistent with the previous studies where imatinib and its derivatives were tested on A549 cells [28,29] and with studies in other cells and tissues [69]. A study by Khan et al (2016) investigated the effect of imatinib-loaded nanoparticles in various glioma and glioblastoma cell lines, and they showed a decrease by more than half in imatinib's IC_{50} when cells were treated with IMA-NPs [70]. The study by Benny et al (2009) also measured the effect of their imatinib-loaded PLGA microspheres on glioma and glioblastoma cells and found that cell viability was decreased by 57 % to 65 % when treated with imatinib released from PLGA microspheres over twelve days. As established earlier, imatinib is released much more slowly from these NPs because of their size and fabrication method. This reduction of live cells was also reflected here in our study when the cells were treated with imatinib-loaded NPs, both using PLGA 50:50 or PLGA 75:25 (F6 and F8), showing that the lactic/glycolic ratio in PLGA did not significantly affect the release and effect of imatinib on A549 cells. This lack of difference was also found in the study by Karal-Yilmaz et al (2016), looking at imatinib-loaded microspheres for craniopharyngioma where PLGA 75:25 and 50:50 exhibited the same effect for up to 10 days [11]. Blank PLGA-treated cells led to no changes in the population of live cells as expected due to PLGA being a biodegradable and non-toxic polymer [71].

Imatinib may exert its anti-proliferative effect by targeting intracellular tyrosine kinase proteins [1]. The PLGA NPs obtained in this study have been shown to safely deliver imatinib into the cells and exert these effects without needing cell transporters but via endocytosis. Indeed, many studies have hypothesised that PLGA NPs' uptake occurs via endocytosis or receptor-mediated endocytosis [72–74]. For instance, Yin & Feng (2005) established that the endocytosis of PLGA NPs was size-dependent, with the highest uptake seen for NPs between 100 and 500 nm, suggesting that the NPs produced in this study (400–500 nm) would also be taken up via endocytosis [75]. Panyam & Labhasetwar (2002) and Yin & Feng (2005) both demonstrated that the uptake was also time-dependent with an increase in intracellular NPs as early as within 1 min post-treatment in smooth muscle cells and 30 min in colon epithelial cells (Caco-2 cells) and kept increasing in the presence of NPs in the media [72,75]. Rhodamine-B has been used previously as a model drug to investigate the cellular uptake of PLGA NPs in epithelial cells to deliver RNAi material and has shown that the rate of uptake of Rhodamine-B-loaded NPs into cells is cell-dependent, varying from 6 to 24 h [76]. A study on Docetaxel-loaded PLGA NPs investigated the NP uptake in A549 cells and found that high cellular uptake was achieved by 6 h. The overexpression of caveolin-1, a cell surface protein, in lung cancer cells has also been found to cause an increase in NP uptake, which demonstrates the caveolin-mediated endocytosis of the PLGA NPs in A549 cells [74,77]. The fast and suggested protein-mediated cellular uptake displayed in these studies ensures that the NPs and the payload are delivered intracellularly within the 24-hour incubation time set in our study. Khan et al. (2016), comparing imatinib's relative IC50 in IMA-NPs to free imatinib, attributed the decrease in IC_{50} by IMA-NPs to the improved cellular uptake of the NPs and, therefore, better uptake of imatinib when it has been encapsulated in PLGA, showing consistency with the results presented here [70]. Imatinib resistance has been reported in the treatment of chronic myeloid leukaemia (CML), and an uptake study using radiolabelled imatinib has shown that this resistance could be due to the dysfunction of cell transporters responsible for the influx and efflux of imatinib into cells [78]. This further indicates the need for an intracellular carrier to safely deliver imatinib into the cells

and exert its antiproliferative effects. The PLGA NPs obtained in this study can do this without cell transporters.

5. Conclusion

The present study has shown the versatility of electrospraying, its ability to produce a wide range of imatinib-loaded NPs and its high control over the payload's release by changing the technique's parameters. Electrospraying, therefore, shows high potential in encapsulating a wide range of active ingredients and gaining control over their physiochemical characteristics and release profiles while yielding uniform and spherical NPs. The change in formulations has indeed demonstrated the ability to control the size of the nanoparticles while maintaining their uniformity, and imatinib was shown to be incorporated in the NPs using FTIR spectroscopy. The tunability in producing these NPs, generated by a single-step electrospraying technique for the first time, enabled the high encapsulation of imatinib and its controlled release. The resulting imatinib-loaded NPs have been shown to possess efficacy in an in vitro cell-based assay, with a comparable capacity to inhibit A549 cell proliferation as free imatinib. It was also shown that the effect of imatinib on A549 cells was maintained when it was encapsulated in either PLGA 50:50 or 75:25 NPs. The uptake of the NPs by A549 cell cultures was also successfully demonstrated using rhodamine B-loaded NPs. In conclusion, this work has shown great prospects for the passive delivery of imatinib in managing proliferative conditions, whereby its encapsulation and controlled release from NPs may enhance its efficacy and safety. The work also opens the potential for the surface functionalisation of the NPs for more active drug delivery.

CRediT authorship contribution statement

Scheilly L. Tsilova: Writing – original draft, Validation, Methodology, Investigation, Formal analysis, Data curation, Conceptualization. **Benjamin E. Schreiber:** Writing – review & editing, Supervision, Investigation, Conceptualization. **Rebecca Lever:** Writing – review & editing, Validation, Supervision, Methodology, Investigation, Conceptualization. **Maryam Parhizkar:** Writing – review & editing, Supervision, Resources, Project administration, Investigation, Conceptualization.

Declaration of competing interest

The authors declare that they have no known competing financial interests or personal relationships that could have appeared to influence the work reported in this paper.

Data availability

Data will be made available on request.

References

[1] N. Iqbal, N. Iqbal, Imatinib: a breakthrough of targeted therapy in cancer, Chemother Res. Pract. (2014) 1–9, https://doi.org/10.1155/2014/357027.

[2] R.L. Jones, I.R. Judson, The development and application of imatinib, Expert Opin. Drug Saf. 4 (2005) 183–191, https://doi.org/10.1517/14740338.4.2.183.

[3] N.Ü. Okur, P.I. Siafaka, E.H. Gökçe, Challenges in oral drug delivery and applications of lipid nanoparticles as potent oral drug carriers for managing cardiovascular risk factors, Curr. Pharm. Biotechnol. 22 (2020) 892–905, https://doi.org/10.2174/1389201021666200804155535.

[4] B. Gupta, B.K. Poudel, S. Pathak, J.W. Tak, H.H. Lee, J.H. Jeong, H.G. Choi, C. S. Yong, J.O. Kim, Effects of formulation variables on the particle size and drug encapsulation of imatinib-loaded solid lipid nanoparticles, AAPS PharmSciTech 17 (2016) 652–662, https://doi.org/10.1208/S12249-015-0384-Z/TABLES/9.

[5] Novartis Pharmaceuticals, Imatinib (QTI571) in Pulmonary Arterial Hypertension, ClinicalTrials.Gov (2011). https://clinicaltrials.gov/ct2/show/study/NCT00902174 (accessed June 29, 2022).

[6] Y. Wei, L. Zhao, Passive lung-targeted drug delivery systems via intravenous administration, Pharm. Dev. Technol. 19 (2014) 129–136, https://doi.org/10.3109/10837450.2012.757782.

[7] M.R. Molaahmadi, J. Varshosaz, S. Taymouri, V. Akbari, Lipid Nanocapsules for imatinib delivery: design, optimization and evaluation of anticancer activity against melanoma cell line, Iranian Journal of Pharmaceutical Research 18 (2019) 1676–1693, https://doi.org/10.22037/ijpr.2019.1100870.

[8] Y. Nakamura, A. Mochida, P.L. Choyke, H. Kobayashi, Nano-drug delivery: Is the enhanced permeability and retention (EPR) effect sufficient for curing cancer? Bioconjug. Chem. 27 (2016) 2225, https://doi.org/10.1021/ACS.BIOCONJCHEM.6B00437.

[9] H. Makadia, S. Siegel, Poly Lactic-co-Glycolic Acid (PLGA) as biodegradable controlled drug delivery carrier, Polymers (Basel) 3 (2011) 1377–1397, https://doi.org/10.3390/polym3031377.

[10] O. Benny, L.G. Menon, G. Ariel, E. Goren, S.K. Kim, C. Stewman, P.M. Black, R. S. Carroll, M. Machluf, Local delivery of poly lactic-co-glycolic acid microspheres containing imatinib mesylate inhibits intracranial xenograft glioma growth, Clin. Cancer Res. 15 (2009) 1222–1231, https://doi.org/10.1158/1078-0432.CCR-08-1316.

[11] O. Karal-Yilmaz, A. Ozkan, E. Akgun, M. Kukut, K. Baysal, T. Avsar, T. Kilic, Controlled release of imatinib mesylate from PLGA microspheres inhibit craniopharyngioma mediated angiogenesis, J. Mater. Sci. - Mater. Med. 24 (2013) 147–153, https://doi.org/10.1007/S10856-012-4784-2/FIGURES/3.

[12] M. Esfandyari-Manesh, M. Abdi, A.H. Talasaz, S.M. Ebrahimi, F. Atyabi, R. Dinarvand, S2P peptide-conjugated PLGA-Maleimide-PEG nanoparticles containing Imatinib for targeting drug delivery to atherosclerotic plaques, DARU Journal of Pharmaceutical Sciences 28 (2020) 131–138, https://doi.org/10.1007/s40199-019-00324-w.

[13] S. Akagi, K. Nakamura, D. Miura, Y. Saito, H. Matsubara, A. Ogawa, T. Matoba, K. Egashira, H. Ito, Delivery of imatinib-incorporated nanoparticles into lungs suppresses the development of monocrotaline-induced pulmonary arterial hypertension, Int. Heart J. 56 (2015) 354–359, https://doi.org/10.1536/ihj.14-338.

[14] B. Almería, W. Deng, T.M. Fahmy, A. Gomez, Controlling the morphology of electrospray-generated PLGA microparticles for drug delivery, J. Colloid Interface Sci. 343 (2010) 125–133, https://doi.org/10.1016/j.jcis.2009.10.002.

[15] C. Chen, W. Liu, P. Jiang, T. Hong, Coaxial electrohydrodynamic atomization for the production of drug-loaded micro/nanoparticles, Micromachines (Basel) 10 (2019), https://doi.org/10.3390/mi10020125.

[16] T.J. Gutiérrez, Polymers for food applications: news, Polymers for Food Applications (2018) 1–4, https://doi.org/10.1007/978-3-319-94625-2_1/COVER.

[17] M.P. Prabhakaran, M. Zamani, B. Felice, S. Ramakrishna, Electrospraying technique for the fabrication of metronidazole contained PLGA particles and their release profile, Mater. Sci. Eng. C 56 (2015) 66–73, https://doi.org/10.1016/J.MSEC.2015.06.018.

[18] M. Parhizkar, P.J.T. Reardon, J.C. Knowles, R.J. Browning, E. Stride, P.R. Barbara, A.H. Harker, M. Edirisinghe, Electrohydrodynamic encapsulation of cisplatin in poly (lactic-co-glycolic acid) nanoparticles for controlled drug delivery, Nanomedicine 12 (2016) 1919–1929, https://doi.org/10.1016/J.NANO.2016.05.005.

[19] J. Xie, J.C.M. Marijnissen, C.H. Wang, Microparticles developed by electrohydrodynamic atomization for the local delivery of anticancer drug to treat C6 glioma in vitro, Biomaterials 27 (2006) 3321–3332, https://doi.org/10.1016/J.BIOMATERIALS.2006.01.034.

[20] M. Chatterjee, R. Maity, S. Das, N. Mahata, B. Basu, N. Chanda, Electrospray-based synthesis of fluorescent poly(d, l -lactide- co -glycolide) nanoparticles for the efficient delivery of an anticancer drug and self-monitoring its effect in drug-resistant breast cancer cells, Mater Adv 1 (2020) 3033–3048, https://doi.org/10.1039/D0MA00646G.

[21] A.Í.S. Morais, E.G. Vieira, S. Afewerki, R.B. Sousa, L.M.C. Honorio, A.N.C. O. Cambrussi, J.A. Santos, R.D.S. Bezerra, J.A.O. Furtini, E.C. Silva-Filho, T. J. Webster, A.O. Lobo, Fabrication of polymeric microparticles by electrospray: the impact of experimental parameters, J Funct Biomater 11 (2020), https://doi.org/10.3390/jfb11010004.

[22] D.J. Burgess, A.S. Hussain, T.S. Ingallinera, M.L. Chen, Assuring quality and performance of sustained and controlled release parenterals: AAPS workshop report, co-sponsored by FDA and USP, Pharm. Res. 19 (2002) 1761–1768, https://doi.org/10.1023/A:1020730102176/METRICS.

[23] N. Faisant, J. Akiki, F. Siepmann, J.P. Benoit, J. Siepmann, Effects of the type of release medium on drug release from PLGA-based microparticles: Experiment and theory, Int. J. Pharm. 314 (2006) 189–197, https://doi.org/10.1016/J.IJPHARM.2005.07.030.

[24] A. Platel, R. Carpentier, E. Becart, G. Mordacq, D. Betbeder, F. Nesslany, Influence of the surface charge of PLGA nanoparticles on their in vitro genotoxicity, cytotoxicity, ROS production and endocytosis, J. Appl. Toxicol. 36 (2016) 434–444, https://doi.org/10.1002/JAT.3247.

[25] Marcos Luciano Bruschi, Mathematical models of drug release, in: Marcos Luciano Bruschi (Ed.), Strategies to Modify the Drug Release from Pharmaceutical Systems, Elsevier, 2015: pp. 63–86. doi: 10.1016/B978-0-08-100092-2.00005-9.

[26] S. Azadi, H. Ashrafi, A. Azadi, Mathematical modeling of drug release from swellable polymeric nanoparticles, J Appl Pharm Sci 7 (2017) 125–133, https://doi.org/10.7324/JAPS.2017.70418.

[27] DASH SUVAKANTA, NARASIMHA MURTHY ADALA, NATH LILAKANTA, Prasanta Chowdhury, Kinetic modeling on drug release from controlled drug delivery systems, Acta Poloniae Pharmaceutica - Drug Research 67 (2010) 217–223.

[28] S. Chen, L. He, X. Wang, X. Gong, H. Zhang, Synthesis and cytotoxic activity of imatinib derivatives, Chin. J. Org. Chem. 35 (2015) 2377, https://doi.org/10.6023/CJOC201506030.

[29] A. Oliveira, S. Moura, L. Pimentel, J. Neto, R. Dantas, F. Silva, M. Bastos, N. Boechat, New Imatinib Derivatives with Antiproliferative Activity against A549 and K562 Cancer Cells, Molecules 2022, Vol. 27, Page 750 27 (2022) 750. doi: 10.3390/MOLECULES27030750.
[30] S. Castro Coelho, B. Nogueiro Estevinho, F. Rocha, Encapsulation in food industry with emerging electrohydrodynamic techniques: Electrospinning and electrospraying – a review, Food Chem. 339 (2021) 127850, https://doi.org/10.1016/j.foodchem.2020.127850.
[31] J. Anu Bhushani, C. Anandharamakrishnan, Electrospinning and electrospraying techniques: potential food based applications, Trends Food Sci. Technol. 38 (2014) 21–33, https://doi.org/10.1016/j.tifs.2014.03.004.
[32] S.L. Shenoy, W.D. Bates, H.L. Frisch, G.E. Wnek, Role of chain entanglements on fiber formation during electrospinning of polymer solutions: good solvent, non-specific polymer–polymer interaction limit, Polymer (Guildf) 46 (2005) 3372–3384, https://doi.org/10.1016/J.POLYMER.2005.03.011.
[33] R. Festag, S.D. Alexandratos, D.C. Joy, B. Wunderlich, B. Annis, K.D. Cook, Effects of molecular entanglements during electrospray of high molecular weight polymers, J. Am. Soc. Mass Spectrom. 9 (1998) 299–304, https://doi.org/10.1016/S1044-0305(98)00004-X.
[34] V.M. Giménez, N. Sperandeo, S. Faudone, S. Noriega, W. Manucha, D. Kassuha, Preparation and characterization of bosentan monohydrate/ε-polycaprolactone nanoparticles obtained by electrospraying, Biotechnol. Prog. 35 (2019) e2748.
[35] A. Jaworek, A.T. Sobczyk, Electrospraying route to nanotechnology: an overview, J. Electrostat. 66 (2008) 197–219, https://doi.org/10.1016/J.ELSTAT.2007.10.001.
[36] S.K. Boda, X. Li, J. Xie, Electrospraying an enabling technology for pharmaceutical and biomedical applications: a review, J. Aerosol Sci 125 (2018) 164–181, https://doi.org/10.1016/j.jaerosci.2018.04.002.
[37] F. Ito, H. Fujimori, H. Honnami, H. Kawakami, K. Kanamura, K. Makino, Study of types and mixture ratio of organic solvent used to dissolve polymers for preparation of drug-containing PLGA microspheres, Eur. Polym. J. 45 (2009) 658–667, https://doi.org/10.1016/J.EURPOLYMJ.2008.12.037.
[38] M. Trotta, R. Cavalli, C. Trotta, R. Bussano, L. Costa, Electrospray technique for solid lipid-based particle production, Drug Dev. Ind. Pharm. 36 (2010) 431–438, https://doi.org/10.3109/03639040903241817.
[39] H. Horibe, Y. Sasaki, H. Oshiro, Y. Hosokawa, A. Kono, S. Takahashi, T. Nishiyama, Quantification of the solvent evaporation rate during the production of three PVDF crystalline structure types by solvent casting, Polym. J. 46 (2014) 104–110, https://doi.org/10.1038/pj.2013.75.
[40] J. Yao, L. Kuang Lim, J. Xie, J. Hua, C.H. Wang, Characterization of electrospraying process for polymeric particle fabrication, J. Aerosol Sci 39 (2008) 987–1002, https://doi.org/10.1016/J.JAEROSCI.2008.07.003.
[41] J.A. Tapia-Hernández, F. Rodríguez-Félix, I. Katouzian, Nanocapsule formation by electrospraying, Nanoencapsulation Technologies for the Food and Nutraceutical Industries (2017) 320–345, https://doi.org/10.1016/B978-0-12-809436-5.00009-4.
[42] F. Meng, Y. Jiang, Z. Sun, Y. Yin, Y. Li, Electrohydrodynamic liquid atomization of biodegradable polymer microparticles: effect of electrohydrodynamic liquid atomization variables on microparticles, J. Appl. Polym. Sci. 113 (2009) 526–534, https://doi.org/10.1002/APP.30107.
[43] Y. Xu, M.A. Hanna, Electrospray encapsulation of water-soluble protein with polylactide: effects of formulations on morphology, encapsulation efficiency and release profile of particles, Int. J. Pharm. 320 (2006) 30–36, https://doi.org/10.1016/J.IJPHARM.2006.03.046.
[44] J. Wang, J.A. Jansen, F. Yang, Electrospraying: Possibilities and challenges of engineering carriers for biomedical applications - a mini review, Front. Chem. 7 (2019) 258, https://doi.org/10.3389/fchem.2019.00258.
[45] WANG, Introduction to electrospinning, Woodhead Pub, Oxford ; Cambridge :, 2011. doi: 10.1533/9780857092915.1.3.
[46] Y. Cao, B. Wang, Y. Wang, D. Lou, Polymer-controlled core–shell nanoparticles: a novel strategy for sequential drug release, RSC Adv. 4 (2014) 30430–30439, https://doi.org/10.1039/C4RA03610G.
[47] S. Bhattacharya, Fabrication and characterization of chitosan-based polymeric nanoparticles of Imatinib for colorectal cancer targeting application, Int. J. Biol. Macromol. 151 (2020) 104–115, https://doi.org/10.1016/J.IJBIOMAC.2020.02.151.
[48] M. Veverka, P. Šimon, J. Lokaj, E. Veverková, Crystal habit modifications of imatinib mesylate under various precipitation conditions, Monatsh. Chem. 143 (2012) 65–71, https://doi.org/10.1007/S00706-011-0562-Y/TABLES/1.
[49] K. Fu, K. Griebenow, L. Hsieh, A.M. Klibanov, R. Langer, FTIR characterization of the secondary structure of proteins encapsulated within PLGA microspheres, J. Control. Release 58 (1999) 357–366, https://doi.org/10.1016/S0168-3659(98)00192-8.
[50] N.J. Roos, R.V. Mancuso, G.M. Sanvee, J. Bouitbir, S. Krähenbühl, Imatinib disturbs lysosomal function and morphology and impairs the activity of mTORC1 in human hepatocyte cell lines, Food Chem. Toxicol. 162 (2022), https://doi.org/10.1016/J.FCT.2022.112869.
[51] F. Ramazani, W. Chen, C.F. Van Nostrum, G. Storm, F. Kiessling, T. Lammers, W. E. Hennink, R.J. Kok, Strategies for encapsulation of small hydrophilic and amphiphilic drugs in PLGA microspheres: state-of-the-art and challenges, Int. J. Pharm. 499 (2016) 358–367, https://doi.org/10.1016/J.IJPHARM.2016.01.020.
[52] Z. Liu, H. Chen, F. Lv, J. Wang, S. Zhao, Y. Li, X. Xue, Y. Liu, G. Wei, W. Lu, Sequential release of paclitaxel and imatinib from core–shell microparticles prepared by coaxial electrospray for vaginal therapy of cervical cancer, Int. J. Mol. Sci. 22 (2021), https://doi.org/10.3390/ijms22168760.
[53] V. Senthil Kumar, N. Irfan, T.V.A. Kumar, V. Parthasarathy, Assessing the molecular interaction between poly lactic-co-glycolic acid (PLGA) 50: 50 and poly ethylene glycol in presence of diethyl phthalate using in silico study-A novel approach of pre-formulation study, J Pharm Res Int 33 (2021) 144–150, https://doi.org/10.9734/JPRI/2021/v33i52B33610.
[54] H. Valo, L. Peltonen, S. Vehviläinen, M. Karjalainen, R. Kostiainen, T. Laaksonen, J. Hirvonen, Electrospray encapsulation of hydrophilic and hydrophobic drugs in poly(L-lactic acid) nanoparticles, Small 5 (2009) 1791–1798, https://doi.org/10.1002/SMLL.200801907.
[55] X. Huang, C.S. Brazel, On the importance and mechanisms of burst release in matrix-controlled drug delivery systems, J. Control. Release 73 (2001) 121–136, https://doi.org/10.1016/S0168-3659(01)00248-6.
[56] S. Fredenberg, M. Wahlgren, M. Reslow, A. Axelsson, The mechanisms of drug release in poly(lactic-co-glycolic acid)-based drug delivery systems—a review, Int. J. Pharm. 415 (2011) 34–52, https://doi.org/10.1016/J.IJPHARM.2011.05.049.
[57] N. Kamaly, B. Yameen, J. Wu, O.C. Farokhzad, Degradable controlled-release polymers and polymeric nanoparticles: mechanisms of controlling drug release, Chem. Rev. 116 (2016) 2602–2663, https://doi.org/10.1021/ACS.CHEMREV.5B00346/ASSET/IMAGES/LARGE/CR-2015-00346D_0038.JPEG.
[58] H. Okada, H. Toguchi, Biodegradable microspheres in drug delivery, Critical Reviews™ in Therapeutic Drug Carrier Systems 12 (1995) 1–99, https://doi.org/10.1615/CRITREVTHERDRUGCARRIERSYST.V12.I1.10.
[59] L. Ahmed, R. Atif, T. Salah Eldeen, I. Yahya, A. Omara, M. Eltayeb, Study the Using of Nanoparticles as Drug Delivery System Based on Mathematical Models for Controlled Release, International Journal of Latest Technology in Engineering VIII (2019). www.ijltemas.in (accessed May 31, 2024).
[60] R.W. Korsmeyer, R. Gurny, E. Doelker, P. Buri, N.A. Peppas, Mechanisms of solute release from porous hydrophilic polymers, Int. J. Pharm. 15 (1983) 25–35, https://doi.org/10.1016/0378-5173(83)90064-9.
[61] Z. Esmaili, S. Bayrami, F.A. Dorkoosh, H. Akbari Javar, E. Seyedjafari, S. S. Zargarian, V. Haddadi-Asl, Development and characterization of electrosprayed nanoparticles for encapsulation of Curcumin, J Biomed Mater Res A 106 (2018) 285–292, https://doi.org/10.1002/JBM.A.36233.
[62] C. Berkland, M. King, A. Cox, K. Kim, D.W. Pack, Precise control of PLG microsphere size provides enhanced control of drug release rate, J. Control. Release 82 (2002) 137–147, https://doi.org/10.1016/S0168-3659(02)00136-0.
[63] T.-W. Chung, Y.-L. Tsai, J.-H. Hsieh, W.-J. Tsai, W. Chung, Different ratios of lactide and glycolide in PLGA affect the surface property and protein delivery characteristics of the PLGA microspheres with hydrophobic additives, Journal of Microencapsulation Micro and Nano Carriers 23 (2008) 15–27, https://doi.org/10.1080/02652040500286110.
[64] L. Fan, S.K. Singh, Controlled release, Controlled Release (1989), https://doi.org/10.1007/978-3-642-74507-2.
[65] E. Lagreca, V. Onesto, C. Di Natale, S. La Manna, P.A. Netti, R. Vecchione, Recent advances in the formulation of PLGA microparticles for controlled drug delivery, Progress in Biomaterials 2020 9:4 9 (2020) 153–174. doi: 10.1007/S40204-020-00139-Y.
[66] P.W. Manley, S.W. Cowan-Jacob, E. Buchdunger, D. Fabbro, G. Fendrich, P. Furet, T. Meyer, J. Zimmermann, Imatinib: a selective tyrosine kinase inhibitor, Eur. J. Cancer 38 (2002) S19–S27, https://doi.org/10.1016/S0959-8049(02)80599-8.
[67] J. Zhou, Y. Zhang, R. Wang, Controllable loading and release of nanodrugs in polymeric vesicles, Giant 12 (2022) 100126, https://doi.org/10.1016/J.GIANT.2022.100126.
[68] Y. Zhang, T. Shams, A.H. Harker, M. Parhizkar, M. Edirisinghe, Effect of copolymer composition on particle morphology and release behavior in vitro using progesterone, Mater. Des. 159 (2018) 57–67, https://doi.org/10.1016/J.MATDES.2018.08.024.
[69] L. Samei, P. Yaling, Y. Lihua, Z. Yan, J. Shuyan, Effects and mechanism of imatinib in inhibiting colon cancer cell proliferation, Med. Sci. Monit. 22 (2016) 4126, https://doi.org/10.12659/MSM.898152.
[70] A.M. Khan, F.J. Ahmad, A.K. Panda, S. Talegaonkar, Investigation of imatinib loaded surface decorated biodegradable nanocarriers against glioblastoma cell lines: intracellular uptake and cytotoxicity studies, Int. J. Pharm. 507 (2016) 61–71, https://doi.org/10.1016/J.IJPHARM.2016.05.008.
[71] D.N. Kapoor, A. Bhatia, R. Kaur, R. Sharma, G. Kaur, S. Dhawan, PLGA: a unique polymer for drug delivery, Ther. Deliv. 6 (2015) 41–58, https://doi.org/10.4155/tde.14.91.
[72] J. Panyam, V. Labhasetwar, Dynamics of endocytosis and exocytosis of poly(D, L-lactide-co-glycolide) nanoparticles in vascular smooth muscle cells, Pharm. Res. 20 (2003) 212–220, https://doi.org/10.1023/A:1022219003551.
[73] M.G. Qaddoumi, H. Ueda, J. Yang, J. Davda, V. Labhasetwar, V.H.L. Lee, The characteristics and mechanisms of uptake of PLGA nanoparticles in rabbit conjunctival epithelial cell layers, Pharm. Res. 21 (2004) 641–648, https://doi.org/10.1023/B:PHAM.0000022411.47059.76/METRICS.
[74] P. Gupta, A. Singh, A.K. Verma, S. Kant, A.K. Pandey, P. Khare, V. Prakash, The anti-tumor and immunomodulatory effects of PLGA-based docetaxel nanoparticles in lung cancer: the potential involvement of necroptotic cell death through reactive oxygen species and calcium build-up, Vaccines (Basel) 10 (2022), https://doi.org/10.3390/VACCINES10111801/S1.
[75] K. Yin Win, S.S. Feng, Effects of particle size and surface coating on cellular uptake of polymeric nanoparticles for oral delivery of anticancer drugs, Biomaterials 26 (2005) 2713–2722, https://doi.org/10.1016/J.BIOMATERIALS.2004.07.050.

[76] M.S. Cartiera, K.M. Johnson, V. Rajendran, M.J. Caplan, W.M. Saltzman, The uptake and intracellular fate of PLGA nanoparticles in epithelial cells, Biomaterials 30 (2009) 2790–2798, https://doi.org/10.1016/J.BIOMATERIALS.2009.01.057.
[77] L. Simón, A. Campos, L. Leyton, A.F.G. Quest, Caveolin-1 function at the plasma membrane and in intracellular compartments in cancer, Cancer Metastasis Rev. 39 (2020) 435, https://doi.org/10.1007/S10555-020-09890-X.
[78] J. Thomas, L. Wang, R.E. Clark, M. Pirmohamed, Active transport of imatinib into and out of cells: implications for drug resistance, Blood 104 (2004) 3739–3745, https://doi.org/10.1182/BLOOD-2003-12-4276.